

Polaron in a spherical quantum dot embedded in a nonpolar matrix

Kazunori Oshiro, Koji Akai, and Mitsuru Matsuura

*Department of Advanced Materials Science and Engineering, Faculty of Engineering, Yamaguchi University,
Ube, Yamaguchi 755-8611, Japan*

(Received 18 February 1998)

Effects of LO phonons for an electron, confined in a spherical quantum dot embedded in a nonpolar matrix, are studied theoretically. A variational method is used to calculate the polaron energy shift by taking into account the interaction with both the bulk type and the interface type phonons in the system. The combination of the adiabatic and the intermediate coupling methods is developed to provide the results, being valid for the wide range of the dot radius and the electron-phonon coupling strength. The method is applied to GaAs, CdSe, and CuCl quantum dots and the results are discussed in comparison with the second-order perturbation theory and other published theories. General properties of a polaron are also calculated and discussed by changing physical parameters, which characterize the system. It is shown that (i) with the increase in the dot radius the magnitude of the polaron energy shift decreases rapidly from large value and then approaches gradually to the bulk value, and (ii) the bulk type LO phonon has the dominant role for the polaron effects and the contribution of interface LO phonon is very small. [S0163-1829(98)03035-5]

I. INTRODUCTION

Recent remarkable progress in crystal growth technique has made it possible to fabricate semiconductor nanostructures whose characteristic dimensions are of the order of the de Broglie wavelength. Especially the quantum dot system is attracting very much attention in electronic and optical properties.^{1,2}

Electron-phonon coupling effects are very important in electronic and optical properties of polar crystalline materials.³ In the quantum dot system, the role of the electron-phonon interaction on the carrier relaxation has been discussed in paying attention to the dimensional effect.^{4,5} Also, the electron-phonon interaction and the polaron effects have been discussed in a spherical quantum dot,⁶⁻¹² a rectangular quantum box,^{13,14} and a quantum dot with the parabolic potential^{15,16} and in a cylindrical quantum dot.^{17,18} In confined systems, such as quantum well, quantum wire, and quantum dot, longitudinal optical (LO) phonons have their characteristic features, being quite different from the bulk: there exists bulk-type phonons and interface-type phonons.^{6-9,14,15,18-20} To discuss the LO phonon effects on an electron in confined systems, we need to take into account these features for LO phonons.

In a spherical quantum dot, being one of the simplest quantum confined systems, polaron effects of an electron have been investigated with the dielectric continuum model.¹⁰⁻¹² Pan and Pan¹⁰ and Marini *et al.*¹¹ have studied the polaron effects due to both bulk and interface types LO phonons with an adiabatic method. Within their treatment the interface type LO phonons have no contribution to polaron effects. Klimin *et al.*¹² considered the polaron energy shift due to both bulk and interface types LO phonons in GaAs quantum dot with the second-order perturbation theory. They concluded, though details of the calculation were not described, that bulk-type phonons play the dominant role in the polaron energy shift, whose magnitude increases rapidly in the limit of the small radius.

The adiabatic method can be used only for the electronic states that are separated from other states by the energy difference being much larger than the phonon energy. This is satisfied in the present problem for the following two cases. One is the case of the strong electron-phonon interaction, by which an electron localizes strongly. Another is the case of the small radius of the spherical dot, where the energy difference between the electronic states becomes much larger than the phonon energy because the electronic energies are inversely proportional to the square of the dot radius R . Thus the adiabatic method becomes valid.

On the other hand, for the large dot with the weak electron-phonon coupling the situation is quite different: the smaller energy difference between electronic states makes the adiabatic method to be invalid, and the polaron effect due to the electron-LO phonon coupling should be treated with the nonadiabatic approximation such as the intermediate coupling method. In fact, for the large dot, the adiabatic method used by Pan and Pan¹⁰ and Marini *et al.*¹¹ do not yield the bulk polaron energy in the weak electron-phonon coupling region, which will be seen explicitly in the later section of the present work.

In the present work, we study effects of the electron-phonon interaction in a polar spherical quantum dot embedded in a nonpolar matrix. Considering that the previous results¹⁰⁻¹² are valid only for some limited cases, we develop the variational method, being valid for the wide range of the dot radius and the electron-phonon coupling strength. Calculation and discussion of the polaron energy shift are performed to clarify the nature of polaron effects systematically, including the role of the bulk-type and the interface-type phonons.

This paper is organized as follows. In Sec. II with the use of the dielectric continuum model the variational method for the polaron in a spherical quantum dot is developed. In Sec. III the behavior of the polaron at the small dot limit and the large dot limit in both weak and strong electron-phonon coupling cases are analyzed. In order to compare with the other

author's result,¹⁰⁻¹² the polaron energies of GaAs, CdSe, and CuCl quantum dots are calculated numerically. General properties of the polaron effect in this system are also calculated and discussed. The conclusion is given in Sec. IV.

II. THEORY

Let us consider an electron, which is confined perfectly in a sphere with radius R and is interacting with LO phonons. The Hamiltonian of the system is given by

$$H = H_e + H_{\text{ph}} + H_{\text{int}}. \quad (2.1)$$

Here the electronic part H_e is given by

$$H_e = \frac{\mathbf{p}^2}{2m} + V_{\text{conf}}(\mathbf{r}), \quad (2.2)$$

where \mathbf{p} and \mathbf{r} are momentum and position of an electron, respectively. m is electron mass. $V_{\text{conf}}(\mathbf{r})$ is the confinement potential for an electron:

$$V_{\text{conf}}(\mathbf{r}) = \begin{cases} \infty & \text{for } r > R \\ 0 & \text{for } r < R, \end{cases} \quad (2.3)$$

where $r = |\mathbf{r}|$.

The solution of the electronic part is well known and is obtained from the Schrödinger equation $H_e \psi^e(\mathbf{r}) = E^e \psi^e(\mathbf{r})$, which yields the wave function and the energy as follows:

$$\psi_{nlm}^e(\mathbf{r}) = \sqrt{\frac{2}{R^3 j_{l+1}(k_{nl}R)}} j_l(k_{nl}r) Y_l^m(\theta, \varphi), \quad (2.4a)$$

$$E_{nl}^e = \frac{\hbar^2 k_{nl}^2}{2m}.$$

Here the state is specified by the set of quantum numbers (n, l, m) . The functions $j_l(x)$ and $Y_l^m(\theta, \varphi)$ are the spherical Bessel function and the spherical harmonics, respectively. k_{nl} is defined by $k_{nl} = \mu_{ln}/R$, where μ_{ln} is the n th zero of the spherical Bessel function of order l ; $j_l(\mu_{ln}) = 0$. Especially for the ground state $(1, 0, 0)$, μ_{01} is equal to π and then the wave function $\psi_g^e = \psi_{100}^e$ and the energy $E_g^e = E_{10}^e$ are given by, respectively,

$$\psi_g^e(\mathbf{r}) = \sqrt{\frac{\pi}{2R^3}} j_0(\pi r/R) \quad (2.4b)$$

$$E_g^e = \frac{\hbar^2 \pi^2}{2mR^2}.$$

The LO phonon Hamiltonian H_{ph} and the electron-LO phonon interaction Hamiltonian H_{int} are written by^{6,10,11}

$$H_{\text{ph}} = \sum_{s,\sigma} \hbar \omega_{s\sigma} a_{s\sigma}^\dagger a_{s\sigma} \quad (2.5)$$

and

$$H_{\text{int}} = \sum_{s,\sigma} \hbar \omega_{s\sigma} v_{s\sigma} [S_{s\sigma}(\mathbf{r}) a_{s\sigma} + \text{H.c.}], \quad (2.6)$$

respectively, where

$$S_{s1}(\mathbf{r}) = \begin{cases} j_l(k_{nl}r) Y_l^m(\theta, \varphi) & (r \leq R) \\ 0 & (r > R) \end{cases} \quad (2.7)$$

and

$$S_{s2}(\mathbf{r}) = \begin{cases} (r/R)^l Y_l^m(\theta, \varphi) & (r \leq R) \\ (R/r)^{l+1} Y_l^m(\theta, \varphi) & (r > R). \end{cases} \quad (2.8)$$

Here $\sigma = 1$ and 2 denote the bulk-type and the interface-type LO phonon, respectively. Another index s is given by $s = (n = 1, 2, 3, \dots; l = 0, 1, 2, \dots; m = 0, \pm 1, \pm 2, \dots, \pm l)$ for the bulk-type phonon and $s = (l = 1, 2, 3, \dots; m = 0, \pm 1, \pm 2, \dots, \pm l)$ for the interface-type phonon. $a_{s\sigma}^\dagger (a_{s\sigma})$ is the creation (annihilation) operator of the $s\sigma$ mode.

The energy for the bulk-type LO phonon $\hbar \omega_{s1}$ is equal to the bulk LO phonon energy $\hbar \omega_{\text{LO}}$, being independent of the index s . The interface phonon energy $\hbar \omega_{s2}$ is given by

$$\hbar \omega_{s2} = \hbar \omega_{\text{LO}} \equiv \left[\frac{\epsilon_d + (\epsilon_d + \epsilon_0)l}{\epsilon_d + (\epsilon_d + \epsilon_\infty)l} \right]^{1/2} \hbar \omega_{\text{TO}} \quad \text{for any } m, \quad (2.9)$$

where $\hbar \omega_{\text{TO}}$ is the transverse optical phonon energy related with $\hbar \omega_{\text{LO}}$ by the well-known Lyddane-Sachs-Teller relation $\omega_{\text{LO}}^2 / \omega_{\text{TO}}^2 = \epsilon_0 / \epsilon_\infty$. ϵ_0 and ϵ_∞ are the static dielectric constant and the high-frequency dielectric constant, respectively. ϵ_d is the dielectric constant of the nonpolar matrix that surrounds the dot sphere.

For the bulk-type phonon, v_{s1} is written as

$$v_{s1} = \sqrt{\frac{8\pi\alpha_1 R_p}{\mu_{ln}^2 j_{l+1}^2(\mu_{ln}) R}}, \quad (2.10)$$

where R_p is the polaron radius defined as $R_p = \sqrt{\hbar / (2m\omega_{\text{LO}})}$ and α_1 is the dimensionless electron-bulk-type phonon coupling constant, which is defined by

$$\alpha_1 = \frac{e^2}{2R_p \hbar \omega_{\text{LO}}} \left(\frac{1}{\epsilon_\infty} - \frac{1}{\epsilon_0} \right).$$

For the interface type phonon, v_{s2} is written as

$$v_{s2} = \sqrt{\frac{4\pi\alpha_2 R_p}{R}}, \quad (2.11)$$

where α_2 is defined by

$$\alpha_2 = \alpha_2(l) \equiv \alpha_1 \left(\frac{\sqrt{l}\epsilon_\infty}{l\epsilon_0 + (l+1)\epsilon_d} \right)^2 \left(\frac{\hbar \omega_{\text{LO}}}{\hbar \omega_{\text{LO}}} \right)^3.$$

By following Lee-Low-Pines theory, the unitary operator in the electron-LO phonon interaction system is defined as²¹⁻²³

$$U = \exp \left[\sum_{s,\sigma} [F_{s\sigma}^*(\mathbf{r}) a_{s\sigma} - F_{s\sigma}(\mathbf{r}) a_{s\sigma}^\dagger] \right]. \quad (2.12)$$

The transformed Hamiltonian $\tilde{H} = U^{-1} H U$ is given by

$$\tilde{H} = \tilde{H}_0 + \tilde{H}_1 + \tilde{H}_2, \quad (2.13)$$

where \tilde{H}_0 , \tilde{H}_1 , and \tilde{H}_2 are zero-phonon, one-phonon, and two-phonon terms:

$$\begin{aligned} \tilde{H}_0 = & \frac{(\mathbf{p}+\mathbf{j})^2}{2m} + V_{\text{conf}}(\mathbf{r}) + \sum_{s,\sigma} \frac{\hbar^2 |\nabla F_{s\sigma}|^2}{2m} \\ & + \sum_{s,\sigma} \hbar \omega_{s\sigma} |F_{s\sigma}|^2 - \sum_{s,\sigma} \hbar \omega_{s\sigma} [v_{s\sigma} S_{s\sigma} F_{s\sigma} + \text{H.c.}], \end{aligned} \quad (2.14)$$

$$\begin{aligned} \tilde{H}_1 = & -\frac{(\mathbf{p}+\mathbf{j}) \cdot \mathbf{J}}{2m} + \sum_{s,\sigma} \frac{[\nabla^2 F_{s\sigma} a_{s\sigma}^\dagger - \nabla^2 F_{s\sigma}^* a_{s\sigma}]}{2m} \\ & - \sum_{s,\sigma} \hbar \omega_{s\sigma} (F_{s\sigma}^* a_{s\sigma} + F_{s\sigma} a_{s\sigma}^\dagger) \\ & + \sum_{s,\sigma} \hbar \omega_{s\sigma} [v_{s\sigma} S_{s\sigma} a_{s\sigma} + \text{H.c.}], \end{aligned} \quad (2.15)$$

and

$$\begin{aligned} \tilde{H}_2 = & \sum_{s,\sigma} \hbar \omega_{s\sigma} a_{s\sigma}^\dagger a_{s\sigma} \\ & + \frac{1}{2m} \sum_{s,\sigma} \sum_{s',\sigma'} [(\nabla F_{s\sigma})(\nabla F_{s'\sigma'}) a_{s\sigma}^\dagger a_{s'\sigma'}^\dagger \\ & + (\nabla F_{s\sigma}^*)(\nabla F_{s'\sigma'}^*) a_{s\sigma} a_{s'\sigma'} \\ & + (\nabla F_{s\sigma})(\nabla F_{s'\sigma'}^*) a_{s\sigma}^\dagger a_{s'\sigma'} \\ & + (\nabla F_{s\sigma}^*)(\nabla F_{s'\sigma'}) a_{s'\sigma'}^\dagger a_{s\sigma}]. \end{aligned} \quad (2.16)$$

Here, we have used the abbreviations

$$\mathbf{J} = -i\hbar \sum_{s,\sigma} [a_{s\sigma}^\dagger \nabla F_{s\sigma} - a_{s\sigma} \nabla F_{s\sigma}^*]$$

and

$$\mathbf{j} = -\frac{i\hbar}{2} \sum_{s,\sigma} [F_{s\sigma}^* \nabla F_{s\sigma} - F_{s\sigma} \nabla F_{s\sigma}^*]. \quad (2.17)$$

The function $F_{s\sigma}$ is chosen in the following form:

$$F_{s\sigma}(\mathbf{r}) = v_{s\sigma} f_{s\sigma} S_{s\sigma}^*(\mathbf{r}) + v_{s\sigma} g_{s\sigma}. \quad (2.18)$$

As the trial function to the transformed state $|\Psi\rangle$, we choose the product form of the electronic state $|\Phi\rangle$ and the zero-phonon state $|0\rangle$, that is $|\Psi\rangle = |\Phi\rangle|0\rangle$. Then the expectation value of the Hamiltonian is given by

$$E = \langle \Psi | \tilde{H} | \Psi \rangle = \langle \Phi | \tilde{H}_0 | \Phi \rangle. \quad (2.19)$$

The choice of only the first term in the right-hand side of Eq. (2.18), i.e., $F_{s\sigma} = v_{s\sigma} f_{s\sigma} S_{s\sigma}^*(\mathbf{r})$, corresponds to the intermediate electron-phonon coupling method. The intermediate coupling method works well in the larger dot size with the weak and the intermediate electron-phonon coupling, where the electronic energy differences are smaller than the LO phonon energy $\hbar \omega_{s\sigma}$. The choice of only the second term of the right-hand side of Eq. (2.18), i.e., $F_{s\sigma} = v_{s\sigma} g_{s\sigma}$, corre-

sponds to the adiabatic method. The adiabatic method is valid when the relevant electronic state is well separated from other electronic states. This situation is realized in a very small radius of the quantum dot as well as in the strongly localized state due to the strong electron-phonon interaction. Thus $F_{s\sigma}$, given by Eq. (2.18), is expected to yield reasonable results for polaron effects for the wide range of the dot radius and the electron-phonon coupling strength. These points will be clearly seen in analysis and the numerical calculation in the next section.

For simplicity we choose that both $f_{s\sigma}$ and $g_{s\sigma}$ are real and have an inversion symmetry. From the variational conditions $\partial \langle \Phi | \tilde{H} | \Phi \rangle / \partial f_{s\sigma} = 0$ and $\partial \langle \Phi | \tilde{H} | \Phi \rangle / \partial g_{s\sigma} = 0$, we obtain the variational parameters $f_{s\sigma}$ and $g_{s\sigma}$ as

$$f_{s\sigma} = \frac{B_{s\sigma} - A_{s\sigma}^2}{B_{s\sigma} + C_{s\sigma} - A_{s\sigma}^2}, \quad (2.20)$$

$$g_{s\sigma} = \frac{A_{s\sigma} C_{s\sigma}}{B_{s\sigma} + C_{s\sigma} - A_{s\sigma}^2}. \quad (2.21)$$

Here $A_{s\sigma}$, $B_{s\sigma}$, and $C_{s\sigma}$ are defined by

$$A_{s\sigma} = \langle \Phi | S_{s\sigma}(\mathbf{r}) | \Phi \rangle,$$

$$B_{s\sigma} = \langle \Phi | |S_{s\sigma}(\mathbf{r})|^2 | \Phi \rangle$$

and

$$C_{s\sigma} = \frac{\hbar}{2m\omega_{s\sigma}} \langle \Phi | |\nabla S_{s\sigma}(\mathbf{r})|^2 | \Phi \rangle.$$

For the electronic state $|\Phi\rangle$, we choose the product form of ψ_g^e in Eq. (2.4b) and the Gaussian function including a variational parameter β :

$$\Phi(r) = \frac{1}{\sqrt{\mathcal{N}}} j_0(\pi r/R) e^{-\beta r^2}. \quad (2.22)$$

Here \mathcal{N} is a normalization constant, given by $\mathcal{N} = 4\pi \int_0^R dr r^2 j_0^2(\pi r/R) e^{-2\beta r^2}$. The Gaussian function in $\Phi(r)$ describes the nature of the localization of the polaron in the strong electron-LO phonon coupling case.

The polaron energy E is given by the minimization of the expectation value of the energy with respect to the variational parameter β , i.e.,

$$\begin{aligned} E = \min_{\beta} & \left\{ \left\langle \Phi \left| \frac{p^2}{2m} + V_{\text{conf}}(r) \right| \Phi \right\rangle \right. \\ & \left. - \sum_{s,\sigma} \hbar \omega_{s\sigma} v_{s\sigma}^2 \left[\frac{B_{s\sigma}(B_{s\sigma} - A_{s\sigma}^2) + A_{s\sigma}^2 C_{s\sigma}}{B_{s\sigma} + C_{s\sigma} - A_{s\sigma}^2} \right] \right\}. \end{aligned} \quad (2.23)$$

Then the polaron energy shift is defined by

$$\Delta E = E - \left\langle \psi_g^e \left| \frac{p^2}{2m} + V_{\text{conf}}(r) \right| \psi_g^e \right\rangle. \quad (2.24)$$

TABLE I. Values of physical parameters for typical semiconductors dots; electron mass m_e , LO phonon energy of bulk $\hbar\omega_{\text{LO}}$, the static dielectric constant ϵ_0 , the high frequency dielectric constant ϵ_∞ , the lattice constant a , the electron-phonon coupling constant α_1 , and the polaron radius R_p . $\alpha_2(l)$ and $\hbar\omega_{l1}$ are the coupling constant of the electron-interface phonon and the interface phonon energy with mode l , respectively: a dot is surrounded by vacuum ($\epsilon_d=1$) or the Pyrex 1710 ($\epsilon_d=6.0$). Values of material parameters m_e , $\hbar\omega_{\text{LO}}$, ϵ_0 , ϵ_∞ , and a are taken from Ref. 11 for CuCl and CdSe and from Ref. 26 for other materials.

	KBr	TlCl	CuCl	CdSe	ZnS	GaAs
m_e	0.369	0.424	0.504	0.13	0.34	0.067
$\hbar\omega_{\text{LO}}$	20.97	21.464	25.64	26.54	43.18	35.33
ϵ_0	4.52	32.7	7.9	9.3	8	12.4
ϵ_∞	2.39	4.76	3.61	6.1	5.1	10.6
α_1	3.051	2.943	2.460	0.460	0.736	0.070
R_p (Å)	22.19	20.46	17.17	33.23	16.11	40.11
a (Å)	6.59	3.84	5.41	5.2	5.41	5.65
[for $\epsilon_d=1$ (vacuum)]						
$\hbar\omega_{l1}$	18.58	18.55	23.02	25.39	40.91	34.92
$\hbar\omega_{l2}$	18.97	19.14	23.51	25.62	41.36	35.01
$\hbar\omega_{l\infty}$	19.46	19.81	24.08	25.89	41.87	35.11
$\alpha_2(1)$	0.589	0.086	0.452	0.153	0.225	0.039
$\alpha_2(2)$	0.325	0.040	0.235	0.082	0.121	0.021
[for $\epsilon_d=6.0$ (Pyrex 1710)]						
$\hbar\omega_{l1}$	16.34	13.37	19.57	23.32	37.28	33.94
$\hbar\omega_{l2}$	16.61	14.26	20.07	23.66	37.85	34.13
$\hbar\omega_{l\infty}$	17.07	15.53	20.85	24.17	38.72	34.39
$\alpha_2(1)$	0.1350	0.1379	0.1821	0.0557	0.0743	0.0148
$\alpha_2(2)$	0.1284	0.1139	0.1689	0.0533	0.0710	0.0146

III. ANALYSIS AND CALCULATION

A. Weak electron-phonon coupling case

In this case, we expect that the Gaussian function in the electronic wave function plays no role, and then we may set $\beta=0$.

Let us consider the large radius limit, i.e., $R\rightarrow\infty$. In this limit the contribution of the interface phonon is negligible. It is enough to consider bulk-type phonons with large n in the phonon mode $s=(n,l,m)$ and then the relations of $A_{s1}\ll B_{s1}$, $C_{s1}=R_p^2 k_s^2 B_{s1}$ and $v_{s1}=8\pi\alpha_1 R_p/R$ hold. Thus, the variational parameters f_{s1} and g_{s1} in the unitary transformation Eq. (2.12) reduce to

$$f_{s1} = \frac{1}{1+R_p^2 k_s^2} \quad (3.1)$$

and

$$g_{s1} = 0. \quad (3.2)$$

Therefore we have the polaron energy shift:

$$\Delta E = -\hbar\omega_{\text{LO}} \sum_s \frac{v_{s1}^2 B_{s1}}{1+R_p^2 k_s^2}. \quad (3.3)$$

By using the relation between the spherical wave and the plane wave

$$j_l(kr)Y_l^m(\theta, \varphi) = \frac{1}{4\pi i^l} \int d\Omega_{\mathbf{k}} Y_l^{m*}(\theta_k, \varphi_k) e^{i\mathbf{k}\cdot\mathbf{r}}, \quad (3.4)$$

we can show $\sum_{l,m} B_{s1} = 1/4\pi$. Then, by changing the sum over n into the integral of k , ΔE in the large dot limit is obtained as

$$\Delta E = -\hbar\omega_{\text{LO}} \frac{R}{\pi} \int_0^\infty dk \frac{2\alpha_1 R_p}{R} \frac{1}{1+R_p^2 k^2} = -\alpha_1 \hbar\omega_{\text{LO}}, \quad (3.5)$$

which is the well-known polaron energy shift in the weak electron-phonon coupling case in the bulk.^{21,24}

In the small radius limit, we have $C_{s\sigma} \gg A_{s\sigma}$, $B_{s\sigma}$. Thus $f_{s1}=f_{s2}=0$, $g_{s1}=A_{s1}$, and $g_{s2}=0$ are obtained, and then the polaron energy shift ΔE is given by

$$\Delta E = -\hbar\omega_{\text{LO}} \sum_n v_{(n,0,0)1}^2 A_{(n,0,0)1}^2 \approx -\hbar\omega_{\text{LO}} v_{(1,0,0)1}^2 A_{(1,0,0)1}^2, \quad (3.6)$$

which is equal to the result by the adiabatic method.¹¹ We note that the above weak-coupling polaron energy shifts ΔE in the large and small dot limits, given by Eqs. (3.3) and (3.6) can be derived from the second-order perturbation, as shown in the Appendix.

B. Strong electron-phonon coupling case

In the case of the strong electron-phonon interaction an electron localizes at a small region. If the radius of this region is much smaller than the dot radius, the electronic wave function $\Phi(r)$ reduces to $(8\beta^3/\pi^3)^{1/4} \exp(-\beta r^2)$. Then for the large β in a large dot $C_{s1} \gg A_{s1}$, B_{s1} . Thus f_{s1} and f_{s2} are negligible and $g_{s1}=A_{s1}$ and $g_{s2}=0$ in Eq. (2.18) are

obtained. This yields the same results in the adiabatic treatment of Ref. 11. Then the polaron energy E is given by

$$E = \min_{\beta} \left\{ 3\beta R_p^2 \hbar \omega_{LO} - \frac{2\alpha_1 R_p \sqrt{\beta}}{\sqrt{\pi}} \hbar \omega_{LO} \right\}. \quad (3.7)$$

Here the minimum is achieved at $\beta = \alpha_1^2 / (9\pi R_p^2)$ and the polaron energy shift ΔE is given by

$$\Delta E = -\frac{\alpha_1^2}{3\pi} \hbar \omega_{LO}, \quad (3.8)$$

which is the well-known polaron energy shift of the strong electron-phonon coupling system in the bulk.^{24,25}

C. Application to GaAs, CdSe, and CuCl dot systems

It has been shown in the above that the present theory can give correct results in both limits of the weak and the strong electron-phonon coupling cases. Thus, we expect that our method, which combines the adiabatic method and the intermediate coupling method, can give reasonable results in wide regions. To confirm this point and compare our theory with other authors' published theories,¹⁰⁻¹² we compute the polaron energy shift of GaAs, CdSe, and CuCl quantum dot numerically. The physical parameters for the calculation are taken from Ref. 26 for GaAs and from Ref. 11 for CdSe and CuCl, which are given in Table I. We note that the degree of freedom for the bulk-type phonons N is limited in dot system and then the summation over bulk-type phonon mode $s = (n, l, m)$ in the calculation is limited to N , approximately given by the volume of the dot divided by the unit cell volume. However, it is shown that this limitation of sum has little effect on the results as seen below.

First, we discuss polaron energy shift in a GaAs dot, for which numerical results by the second-order perturbation were shown by Klimin *et al.*¹² The calculated polaron energy shifts as a function of the dot radius by the present variational method and the second-order perturbation method are

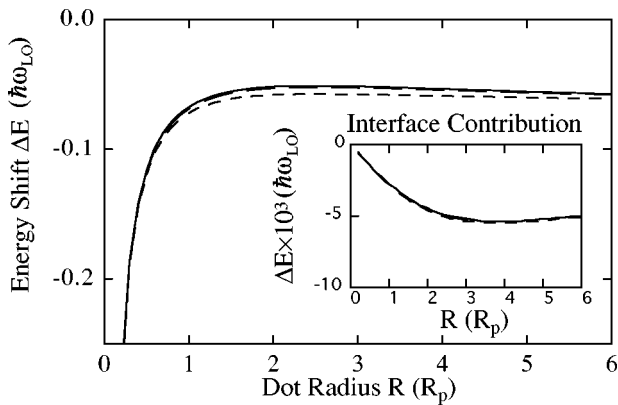


FIG. 1. The polaron energy shift ΔE as a function of the dot radius R for GaAs quantum dot. The solid line stands for the present variational method, the short-dashed line for the variational method without limitation of sum over bulk-type phonon modes s , and the long-dashed line for the the second-order perturbation theory without limitation of sum over bulk-type phonon modes s . In the inset the contribution of the interface type phonon in the polaron energy shift is shown.

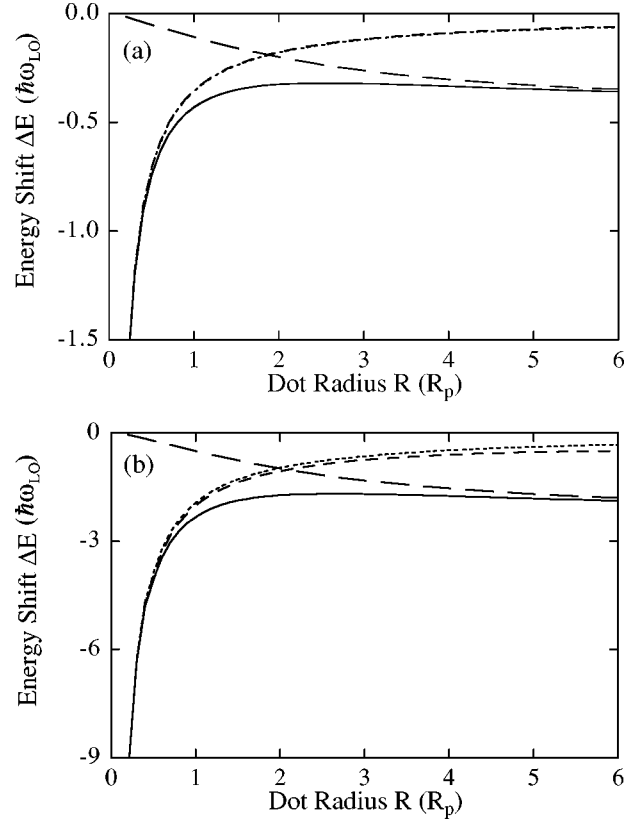


FIG. 2. The polaron energy shift ΔE as a function of the dot radius R in the case of (a) CdSe and (b) CuCl quantum dot. The solid line stands for our variational method, and the long-dashed line for the intermediate coupling method. The dotted line is results of the method of Pan and Pan (Ref. 10), and the short-dashed line is results of the method of Marini *et al.* (Ref. 11).

shown in Fig. 1. In the calculation we take $\epsilon_d = 2$ as in Ref. 12. The solid line is the result of the variational method, the short-dashed line for the variational method without limitation of sum over bulk-type phonon modes s and the long-dashed line shows the result of the second-order perturbation, which is calculated from the following expression:

$$\Delta E^{(2)} = - \sum_{n,l,m} \sum_{s,\sigma} \frac{|\langle \psi_{nlm}^e | \hbar \omega_{s\sigma} v_{s\sigma} S_{s\sigma}(\mathbf{r}) | \psi_g^e \rangle|^2}{E_{nl}^e + \hbar \omega_{s\sigma} - E_g^e}. \quad (3.9)$$

Here the calculation of the second-order perturbation has been performed also without the limitation of the bulk-type phonon modes.

In Fig. 1 we see that the limitation of sum over bulk-type phonon modes yields little effects on the polaron energy shift. One might consider this limitation is effective in the polaron energy shift in the small dot. However, it is noted that the rapid increase of the magnitude of the polaron energy shift for small radius comes from the contribution of only the single bulk-type mode $s = (n = 1, l = 0, m = 0)$.

As GaAs crystal is a weak electron-phonon interaction system, the second-order perturbation theory is considered to work well. As seen in Fig. 1, the difference between results by two methods is small and our variational method gives reasonable results for any dot size. It should be pointed out that Klimin *et al.*¹² calculated the polaron energy shift only

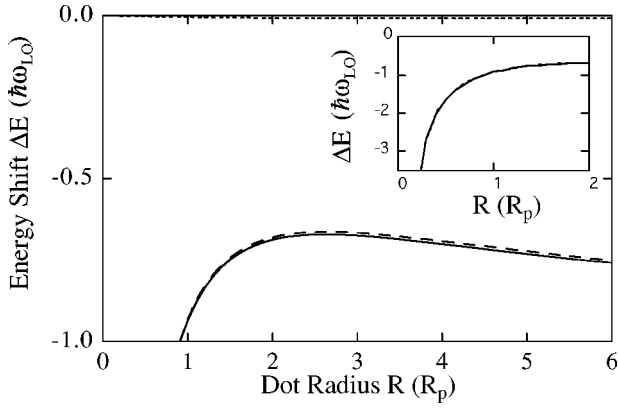


FIG. 3. Contribution of the bulk and the interface phonon for the polaron energy shift ΔE as a function of the dot radius R . The solid line stands for the polaron energy shift ΔE , the dashed line for the contribution of the bulk type phonon, and the dotted line for the contribution of the interface type phonon. The physical parameters are set as $\epsilon_0/\epsilon_\infty=2$, $\epsilon_d/\epsilon_\infty=1.5$, and $\alpha_1=1$. The inset shows the polaron energy shift ΔE in the range of small dot radius R .

for a small radius $r \leq 1.5R_p$. In the region, the magnitude of the polaron energy shift decreases monotonously with the increase of the dot radius. However, it is seen from Fig. 1 that for the further increase of the dot radius, the magnitude of the polaron energy shift reaches to the minimum and then increases gradually to approach the bulk value $\alpha_1 \hbar \omega_{LO}$. The inset in Fig. 1 shows that the contribution of interface-type phonons in the polaron energy shift is very small.

Next we discuss the polaron energy shift in the case of CdSe and CuCl, for which numerical results of the electron-phonon interaction energy were shown in Ref. 11. The calculated polaron energy shifts are shown in Fig. 2. The dotted line in Fig. 2 is the result of the method of Pan and Pan¹⁰ and the short-dashed line is the result of the method of Marini *et al.*¹¹ In both works they used the adiabatic method, which corresponds to the consideration of only the second term in the right-hand side of Eq. (2.18), i.e., $F_{s\sigma} = v_{s\sigma} g_{s\sigma}$. Marini *et al.* included the localization effect of the electronic wave function due to the strong electron-phonon interaction in the same way in Eq. (2.22) and Pan and Pan did not. The long-dashed line is the result of the intermediate coupling method in which only the first term in the right-hand side of Eq. (2.18), $F_{s\sigma} = v_{s\sigma} f_{s\sigma} S_{s\sigma}$, is kept. It is clearly seen that our variational method gives a much better result than the other previous adiabatic methods^{10,11} in all the regions.

It is also clearly seen in Fig. 2 that the inclusion of both the intermediate and the adiabatic terms in $F_{s\sigma}$ is essential to describe the polaron in a spherical quantum dot. This is contrasted with the quantum well system, where only the intermediate term describes well the polaron energy shift for the wide range of the well width.²⁷ The difference arises from the fact that, in quantum-well system, there are continuum free states in the x - y plane even if the well width in the z direction becomes small and, in the quantum dot system, the electronic energy difference becomes much larger than the phonon energy for a small radius. This makes the adiabatic term to be very important for the small dot.

Figures 1 and 2 show that with increasing the dot radius the magnitude of the polaron energy shifts decrease rapidly from a large value, via a minimum and then increase to ap-

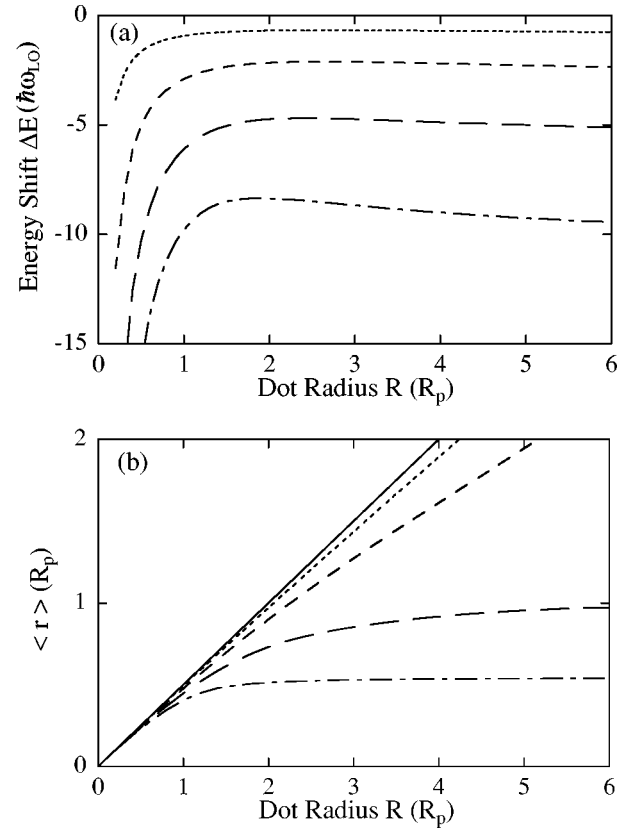


FIG. 4. (a) The polaron energy shift ΔE and (b) the expectation value $\langle r \rangle$ of r as function of the dot radius R , taking the electron bulk type phonon coupling α_1 as a parameter. The dash-dotted line stands for $\alpha_1=9$, the long-dashed line for $\alpha_1=6$, the short-dashed line for $\alpha_1=3$, and the dotted line for $\alpha_1=1$. The solid line stands for $R/2$ in Fig. 4(b). The other physical parameters are set as $\epsilon_0/\epsilon_\infty=2$, $\epsilon_d/\epsilon_\infty=1.5$.

proach gradually to the bulk value. The large magnitude of the polaron energy shift for a smaller dot is due to a existence of an electron even if the dot radius becomes very small, which yields the stronger coupling between an electron and phonon. The gradual increase in the magnitude of the polaron energy shift for the large dot is caused by an increase of the contribution of nonadiabatic processes with increasing the dot radius. These two effects yield a minimum of the magnitude of the polaron energy shift.

D. General properties of the polaron in a spherical dot

Now, changing physical parameters for the system variously, we calculate polaron energy shifts and discuss general properties of the polaron in a spherical quantum dot systematically. The present system is characterized by the following seven physical parameters: electron mass m , the static dielectric constant ϵ_0 , and the high-frequency dielectric constant ϵ_∞ of the inside of the dot, the dielectric constant ϵ_d of the outside of the dot, the bulk LO phonon energy of the dot material $\hbar \omega_{LO}$, the dot radius R , and the lattice constant of the dot material a . Values of these parameters for the typical semiconductors are given in Table I, together with some interface phonon energies and electron-interface coupling constants $\alpha_2(l)$. If we take R_p and $\hbar \omega_{LO}$ as the units of length and energy, then properties of the system are characterized

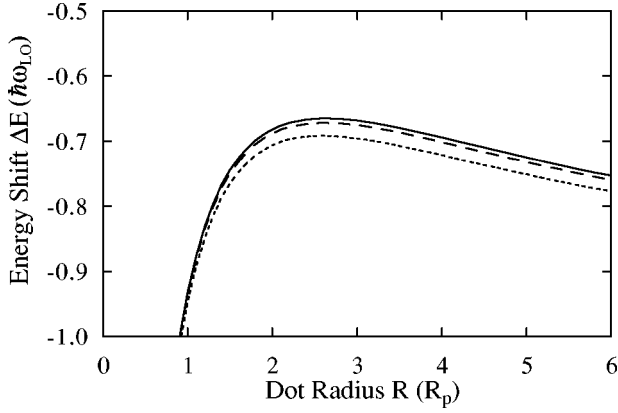


FIG. 5. The polaron energy shift ΔE as a function of the dot radius R , taking the ratio of the dielectric constants $\epsilon_d/\epsilon_\infty$ as a parameter. The solid line stands for $\epsilon_d/\epsilon_\infty=2$, the dashed line for $\epsilon_d/\epsilon_\infty=1.5$, and the dotted line for $\epsilon_d/\epsilon_\infty=1$. The other physical parameters are set as $\epsilon_0/\epsilon_\infty=2$ and $\alpha_1=1$.

by the following five physical parameters: α_1 , $\epsilon_0/\epsilon_\infty$, $\epsilon_d/\epsilon_\infty$, R , and a . We set $a/R_p=0.2$ as a typical value. To discuss general properties of an electron under the influence of the LO phonon the four physical parameters α_1 , $\epsilon_0/\epsilon_\infty$, $\epsilon_d/\epsilon_\infty$, and R are changed in the wide range, while typical values in Table I are kept in mind. The results of numerical calculation of the polaron energy shift are plotted in Figs. 3–5.

To see the role of both bulk- and interface type-phonons for the polaron energy shift, the polaron energy shift ΔE as a function of the dot radius R is plotted in Fig. 3 for the fixed values of $\epsilon_0/\epsilon_\infty=2$, $\epsilon_d/\epsilon_\infty=1.5$, and $\alpha_1=1$. As shown in Fig. 3 the contribution of the interface-type phonon is very much smaller than the contribution of the bulk-type phonon. In passing it is noted that, in interface phonon effects, only the first few terms in the summation of l contribute. This is expected from the values of $\alpha_2(l)$ in Table I together with the limiting value $\alpha_2(\infty)=0$.

In Fig. 4 the polaron energy shifts and the expectation value $\langle r \rangle = \langle \Phi | r | \Phi \rangle$ for the four values of $\alpha_1 = 1, 3, 6,$ and 9 are plotted as a function of the dot radius R , when the values of $\epsilon_0/\epsilon_\infty=2$ and $\epsilon_d/\epsilon_\infty=1.5$ are fixed. In the case of $\alpha_1 = 1$ and 3 the polaron energy shift approaches to $-\alpha_1 \hbar \omega_{LO}$, which is the result of the theory of the weak coupling. On the other hand, for the strong electron-phonon coupling case of $\alpha_1=9$, the polaron energy shift is smaller than $-\alpha_1 \hbar \omega_{LO}$ in $R/R_p \geq 4$. The behavior of $\langle r \rangle$ in Fig. 4(b) shows the importance of the modification effect of the electronic wave function due to the electron-phonon coupling. Without the modification, i.e., with $\beta=0$, we have $\langle r \rangle = R/2$. Thus the deviation from the line of $\langle r \rangle = R/2$ shows the importance of the modification. It is seen that for larger electron-phonon coupling α_1 and the larger dot radius the modification effect becomes important. Especially in the case of $\alpha_1=6$ and 9 the effect becomes large, which reflect the localization of an electron due to the strong electron-phonon coupling.

Figure 5 shows the polaron energy shift as a function of the dot radius R for the three values of $\epsilon_d/\epsilon_\infty = 5.0, 1.5,$ and 0.2 and the fixed values of $\epsilon_0/\epsilon_\infty=2$ and $\alpha_1=1$. It is seen that the ratio $\epsilon_d/\epsilon_\infty$, i.e., the effects of the dielectric constant outside the sphere, has only a small influence upon the polaron energy shift.

IV. CONCLUSION

We have discussed the LO phonon effects of an electron in a spherical quantum dot, embedded in a nonpolar matrix. We take account of both bulk-type and interface-type LO phonons being characteristic in the system. The developed variational method combines the adiabatic method and the intermediate coupling method. The present method has been shown to be valid for the wide range of the dot size and the electron-phonon coupling strength. The above combination is essential to obtain this wide applicability. It is seen in the present wide range of the calculations that the bulk-type phonons have a dominant role and the interface phonons yield only very small effects.

Finally, we mention remaining problems related to the present work. There are many experiments in the quantum dot system whose barrier region has LO phonons, such as a system of a CuCl dot in NaCl crystal. Thus it is necessary to studying the electron-phonon coupling effects in this type of system, for which the present variational method is expected to work well. Also, the present method can be extended to treat the exciton interacting with LO phonons in a spherical quantum dot, whose electronic and optical properties are currently attracting very much attention.

ACKNOWLEDGMENTS

We would like to thank Dr. R. Zheng and Dr. H. Kurisu for useful discussions.

APPENDIX: THE SMALL AND THE LARGE DOT LIMIT IN THE SECOND-ORDER PERTURBATION

In this appendix we discuss the polaron energy shift $\Delta E^{(2)}$ by the second-order perturbation in Eq. (3.9) in the both small and large dot limits.

First we show that Eq. (3.9) reduces to Eq. (3.3) in the large dot limit. We can rewrite $\Delta E^{(2)}$ in Eq. (3.9) in the form²⁸

$$\Delta E^{(2)} = - \sum_{s,\sigma} |\hbar \omega_{s\sigma} v_{s\sigma}|^2 \times \langle \psi_g^e | S_{s\sigma}^* [\hbar \omega_{s\sigma} + H_e - E_g^e]^{-1} S_{s\sigma} | \psi_g^e \rangle. \quad (\text{A1})$$

In the large dot limit the interface phonon contribution can be neglected and then

$$\Delta E^{(2)} = - \sum_{n,l,m} |\hbar \omega_{LO} v_{s1}|^2 \times \langle \psi_g^e | S_{s1}^* [\hbar \omega_{LO} + H_e - E_g^e]^{-1} S_{s1} | \psi_g^e \rangle. \quad (\text{A2})$$

By using the relation between the spherical wave and the plane wave in Eq. (3.4), $\Delta E^{(2)}$ can be written as

$$\Delta E^{(2)} = - \sum_{n,l,m} \frac{|\hbar \omega_{LO} v_{s1}|^2}{(4\pi)^2} \int d\Omega_{\mathbf{k}'} \int d\Omega_{\mathbf{k}} \times Y_l^{m*}(\theta_{\mathbf{k}'}, \varphi_{\mathbf{k}'}) Y_l^m(\theta_{\mathbf{k}}, \varphi_{\mathbf{k}}) \times \langle \psi_g^e | e^{-i\mathbf{k}' \cdot \mathbf{r}} [\hbar \omega_{LO} + H_e - E_g^e]^{-1} e^{i\mathbf{k} \cdot \mathbf{r}} | \psi_g^e \rangle. \quad (\text{A3})$$

Using the relation

$$e^{-i\mathbf{k}\cdot\mathbf{r}}H_e e^{i\mathbf{k}\cdot\mathbf{r}} = \frac{(\mathbf{p} + \hbar\mathbf{k})^2}{2m} + V_{\text{conf}}, \quad (\text{A4})$$

and $H_e|\psi_g^e\rangle = E_g^e|\psi_g^e\rangle$, we obtain

$$\begin{aligned} & [\hbar\omega_{\text{LO}} + H_e - E_g^e]^{-1} e^{i\mathbf{k}\cdot\mathbf{r}} |\psi_g^e\rangle \\ &= e^{i\mathbf{k}\cdot\mathbf{r}} \left[\hbar\omega_{\text{LO}} + \frac{\hbar^2 k_{\text{in}}^2}{2m} + \frac{\hbar\mathbf{k}\cdot\mathbf{p}}{m} + H_e - E_g^e \right]^{-1} |\psi_g^e\rangle \\ &= e^{i\mathbf{k}\cdot\mathbf{r}} \sum_{j=0}^{\infty} \left[\hbar\omega_{\text{LO}} + \frac{\hbar^2 k_{\text{in}}^2}{2m} \right]^{-(j+1)} \left(\frac{\hbar\mathbf{k}\cdot\mathbf{p}}{m} \right)^j |\psi_g^e\rangle. \end{aligned} \quad (\text{A5})$$

Then, keeping the first term in the summation j and using the relation in Eq. (3.4), we can obtain

$$\Delta E^{(2)} = - \sum_{n,l,m} \frac{|\hbar\omega_{\text{LO}} v_{s1}|^2}{\hbar\omega_{\text{LO}} + \hbar^2 k_{\text{in}}^2 / (2m)} \langle \psi_g^e | |S_{s1}|^2 | \psi_g^e \rangle. \quad (\text{A7})$$

This is the result in Eq. (3.3), which yields the bulk polaron energy shift $-\alpha_1 \hbar\omega_{\text{LO}}$.

Next we consider the polaron energy shift $\Delta E^{(2)}$ in the small dot limit. In this limit $|E_{nl}^e - E_g^e| \gg \hbar\omega_{\text{LO}}$ for $(n,l) \neq (1,0)$ and thus from Eq. (3.9) we obtain the polaron energy shift

$$\begin{aligned} \Delta E^{(2)} &= -\hbar\omega_{\text{LO}} \sum_n |v_{(n,0,0)1}|^2 |\langle \psi_g^e | S_{(n,0,0)1} | \psi_g^e \rangle|^2 \\ &\simeq -\hbar\omega_{\text{LO}} |v_{(1,0,0)1}|^2 |\langle \psi_g^e | S_{(1,0,0)1} | \psi_g^e \rangle|^2, \end{aligned} \quad (\text{A8})$$

which is the same result in Eq. (3.6).

-
- ¹A. D. Yoffe, *Adv. Phys.* **42**, 173 (1993).
²U. Woggon and S. V. Gaponenko, *Phys. Status Solidi B* **189**, 285 (1995).
³Y. Toyozawa, in *Excitonic Processes in Solids*, edited by Ueta *et al.* (Springer, Berlin, 1986), p. 203.
⁴U. Bockelman and G. Bastard, *Phys. Rev. B* **42**, 8947 (1990); H. Benisty, C. M. Sotomayor-Torr'es, and C. Weisbuch, *ibid.* **44**, 10 945 (1991).
⁵T. Inoshita and H. Sakaki, *Phys. Rev. B* **46**, 7260 (1992).
⁶M. C. Klein, F. Hache, D. Ricard, and C. Flytzanis, *Phys. Rev. B* **42**, 11 123 (1990).
⁷P. A. Knipp and T. L. Reinecke, *Phys. Rev. B* **46**, 10 310 (1992); **48**, 18 037 (1993), and references therein.
⁸E. Roca, C. Trallero-Giner, and M. Cardona, *Phys. Rev. B* **49**, 13 704 (1994).
⁹R. M. Cruz, S. W. Teitsworth, and M. A. Stroscia, *Phys. Rev. B* **52**, 1489 (1995).
¹⁰J. S. Pan and H. B. Pan, *Phys. Status Solidi* **148**, 129 (1988).
¹¹J. C. Marini, B. Srebe, and E. Kartheuser, *Phys. Rev. B* **50**, 14 302 (1994).
¹²S. N. Klimin, E. P. Plkatilov, and V. M. Fomin, *Phys. Status Solidi B* **184**, 373 (1994).
¹³K. D. Zhu and S. W. Gu, *J. Phys.: Condens. Matter* **4**, 1291 (1992).
¹⁴R. M. Cruz, S. W. Teitsworth and M. A. Stroscia, *Superlattices Microstruct.* **13**, 481 (1993); R. M. Cruz, *ibid.* **16**, 427 (1994); **17**, 307 (1995).
¹⁵M. H. Degane and G. A. Farias, *Phys. Rev. B* **42**, 11 950 (1990).
¹⁶S. Sahoo, *Z. Phys. B* **101**, 97 (1996).
¹⁷P. A. Knipp, T. L. Reinecke, A. Lorke, M. Fricke, and P. M. Petroff, *Phys. Rev. B* **56**, 1516 (1997).
¹⁸W. S. Li and C. Y. Chen, *Physica B* **229**, 375 (1997).
¹⁹L. Wendler, *Phys. Status Solidi B* **129**, 513 (1985).
²⁰N. Mori and T. Ando, *Phys. Rev. B* **40**, 6175 (1989).
²¹T. D. Lee, F. Low, and D. Pines, *Phys. Rev.* **90**, 297 (1953).
²²J. Pollman and H. Büttner, *Phys. Rev. B* **16**, 4480 (1977).
²³M. Matsuura and H. Büttner, *Phys. Rev. B* **21**, 679 (1980).
²⁴J. Callaway, *Quantum Theory of the Solid State* (Academic Press, New York, 1974), p. 656.
²⁵S. I. Pekar and L. M. F. Deigen, *J. Exp. Theor. Phys.* **18**, 481 (1948); S. I. Pekar, *Untersuchungen über die Elektronentheorie der Metalle* (Sdademie Verlag, Berlin, 1954).
²⁶O. Madelung, *Semiconductors-Basic Data*, 2nd revised ed. (Springer, Berlin, 1996).
²⁷R. S. Zheng, S. L. Ban, and X. X. Liang, *J. Phys.: Condens. Matter* **6**, 10 307 (1994).
²⁸S. Wang, H. L. Arora, and M. Matsuura, *Phys. Rev. B* **15**, 3685 (1971).